Evolution of Pacific Ocean and the Sea of Japan populations of the gobiid species, *Pterogobius elapoides* and *Pterogobius zonoleucus*, based on molecular and morphological analyses

Akihito [a], Akishinonomiya Fumihito [b,c], Yuji Ikeda [d], Masahiro Aizawa [d], Takashi Makino [e,1], Yumi Umehara [e], Yoshiaki Kai [f], Yuriko Nishimoto [b,g], Masami Hasegawa [b,e,h], Tetsuji Nakabo [i], Takashi Gojobori [b,e,*]

[a] *The Imperial Residence, 1-1 Chiyoda, Chiyoda-ku, Tokyo 100-0001, Japan*
[b] *The Graduate University for Advanced Studies (SOKENDAI), Shonan Village, Hayama, Kanagawa 240-0193, Japan*
[c] *The University Museum, The University of Tokyo, 7-3-1 Hongo, Bunkyo-ku, Tokyo 113-0033, Japan*
[d] *Imperial Household Agency, 1-1 Chiyoda, Chiyoda-ku, Tokyo 100-8111, Japan*
[e] *Center for Information Biology and DDBJ, National Institute of Genetics, Mishima, Shizuoka 411-8540, Japan*
[f] *Maizuru Fisheries Research Station, Field Science Education and Research Center, Kyoto University, Maizuru 625-0086, Japan*
[g] *The Research Institute of Evolutionary Biology, 2-4-28 Kamiyoga, Setagaya-ku, Tokyo, 158-0098, Japan*
[h] *The Institute of Statistical Mathematics, 4-6-7 Minami-Azabu, Minato-ku, Tokyo, 106-8569, Japan*
[i] *The Kyoto University Museum, Kyoto University, Kyoto, 606-8501, Japan*

ARTICLE INFO

ABSTRACT

Pterogobius elapoides and *Pterogobius zonoleucus* are common free-swimming gobies found in rocky and weedy shores along the temperate coast of Japan. We collected individuals of both species from 23 locations around the coast of Japan and compared the mitochondrial nucleotide sequences of two gene regions, CytB and ND2. Phylogenetic trees constructed using the neighbor-joining, maximum parsimony, and maximum likelihood methods consistently indicated that all 125 samples of the two species, which are collected from a variety of locations in Japan, can be clearly divided into the following four clades: "Pacific *P. elapoides*" (Pa-*ela*), "Sea of Japan *P. elapoides*" (SJ-*ela*), "Pacific *P. zonoleucus*" (Pa-*zon*), and "Sea of Japan *P. zonoleucus*" (SJ-*zon*). These four monophyletic clades were supported with very high bootstrap values. Although Pa-*ela* and SJ-*ela* composed a monophyletic clade, it is noteworthy that the two clades of *P. elapoides* also formed a monophyletic group together with SJ-*zon* with a bootstrap value of 95% and 97% by the maximum likelihood and neighbor-joining methods, respectively. We observed several morphological differences between Pa-*ela* and SJ-*ela*, including; 1) six dark bands on the body in the former versus seven dark bands in the latter and 2) more pectoral-fin rays numbering 21–24 (mode 22) in the latter compared to the former (19–22, mode 21). Furthermore, the scatter plots of scores on principal components 1 and 2 based on the morphometric characters roughly separated the populations from each other. Moreover, we documented the following morphological differences between Pa-*zon* and SJ-*zon* for the first time; 1) six light bands on the body in the former versus five light bands in the latter and 2) the light bands from both eyes forming a complete U-shaped marking on the occipital region occurred in 55% of the specimens in the former versus 16% in the latter. However, no significant differences were found in the morphometric characters between the two populations of *P. zonoleucus*. The estimated divergence time of the two *P. zonoleucus* populations was 15.06±2.72 (mean±1 S.E.) times earlier than that of the two *P. elapoides* populations. However, the morphological differences between the two populations of the former were much smaller than those of the latter. An explanation for this obvious discrepancy between morphological and molecular features is proposed from an evolutionary point of view.

1. Introduction

Four species of the goby genus *Pterogobius* are found in Japan and along the southern coast of Korea: *P. virgo* (Temminck and Schlegel, 1845), *P. elapoides* (Günther, 1871), *P. zacalles* (Jordan and Snyder, 1901), and *P. zonoleucus* (Jordan and Snyder, 1901). Among these four species, *P. elapoides* (Fig. 1) and *P. zonoleucus* (Fig. 2) resemble each other in having more similarly positioned bands on both the head and body than the other two congeneric species. In addition, these two species are almost the same in their geographical distribution and habitats in Japan and along the southern coast of Korea, although there is an ecological difference in adults between *P. elapoides* and *P. zonoleucus*: the former swims solitary near rocky bottoms (Fig. 3A), whereas the latter swims in mid-water in schools (Fig. 3B).

For both *P. elapoides* and *P. zonoleucus*, there have been unsolved problems about their evolutionary intra- and inter-species relationships. For example, *P. elapoides* was originally described by Günther (1871) based on a single specimen, probably from Japan, and his illustration shows seven narrow, dark bands on the body. Then, Jordan and Snyder (1901) described a specimen of *P. elapoides* as a new species called *P. daimio*, owing to it having just six wider, dark bands on its body. Snyder (1912) later recognized that *P. daimio* should have been described as a male of *P. elapoides*.

Almost twenty years later, Tanaka (1931) examined many specimens collected from various localities in Japan, and identified them as *P. elapoides* or *P. daimio* respectively by the presence or absence of a seventh dark band on the body. It was revealed that the specimens with the seventh band were distributed mainly along the Sea of Japan coast, whereas the specimens without the seventh band were distributed along the Pacific coast of central-to-southern Honshu. Specimens from the Seto Inland Sea mostly have an interrupted band or just a spot at the position of the seventh band. Moreover, specimens which showed intermediate color patterns were sometimes found
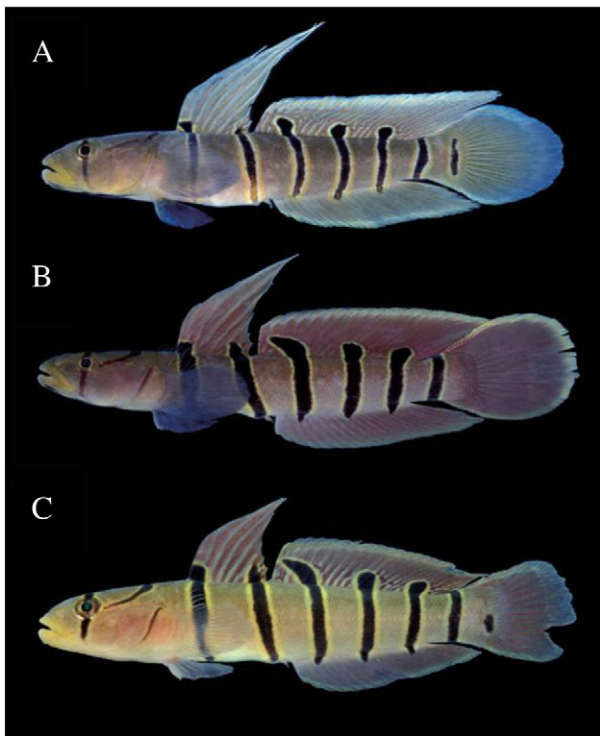

Fig. 1. *Pterogobius elapoides*: (A) The Sea of Japan, Ishikawa Prefecture (BLIH20020439); (B) The Pacific Ocean, Chiba Prefecture (BLIH20030467); (C) The Inland Sea, Ehime Prefecture (BLIH20070130).

Fig. 2. *Pterogobius zonoleucus*: (A) The Sea of Japan, Ishikawa Prefecture (BLIH20050502); (B) The Pacific Ocean, Chiba Prefecture (BLIH20060883).

along the Sea of Japan coast. Because of the presence of intermediate color patterns between *P. elapoides* and *P. daimio*, Tanaka regarded them as a local variation, and recognized the latter as a junior synonym of the former.

Akihito (1984) noted that there are two types of *P. elapoides* which have different geographic distributions: the first type, which has six bands, is found along the Pacific coast of central-to-southern Honshu; the second type, which has seven bands, is found along the coast of Kyushu, the Sea of Japan coast of Honshu and the Sanriku District; in addition, an intermediate type, which has an imperfect seventh band, is found in the Seto Inland Sea. Since then, no detailed morphological and geographical studies of this species have been published. Further, no geographical variation in *P. zonoleucus* has been described in the literature in terms of morphological characters. However, we found some morphological differences between the Sea of Japan and the Pacific Ocean populations.

As no molecular evolutionary studies of *P. elapoides* and *P. zonoleucus* have been published to date, we conducted a molecular phylogenetic analysis on these two species, in addition to morphological studies. From each of 23 sampling localities in the Sea of Japan, Pacific Ocean and the Seto Inland Sea, we collected 5 individuals and sequenced their mtDNA for two genes.

2. Materials and methods

2.1. Samples used (Table 1, Fig. 4)

For *P. elapoides*, 5 individuals were collected at each of 14 different locations in Japan divided equally between the coasts of the Pacific Ocean and the Sea of Japan. For *P. zonoleucus*, 5 individuals were also collected at each of 9 different locations in Japan: 4 locations were along the coast of the Pacific Ocean and 5 locations were along the Sea of Japan (Fig. 4).

For *P. zacalles* and *P. virgo*, which were used as the outgroup in phylogenetic tree construction, 5 individuals for each of the two species were collected from Aomori and Ishikawa Prefectures, respectively. Sampling of these populations was conducted at 2 single locations only. Thus, a total of 125 individuals were sampled from 25 locations along the Pacific Ocean and the Sea of Japan (Table 1).

Abbreviations used in specimen identification numbers are: BLIH — Biological Laboratory, Imperial Household; and NMCI — Noto Marine Center, Ishikawa.
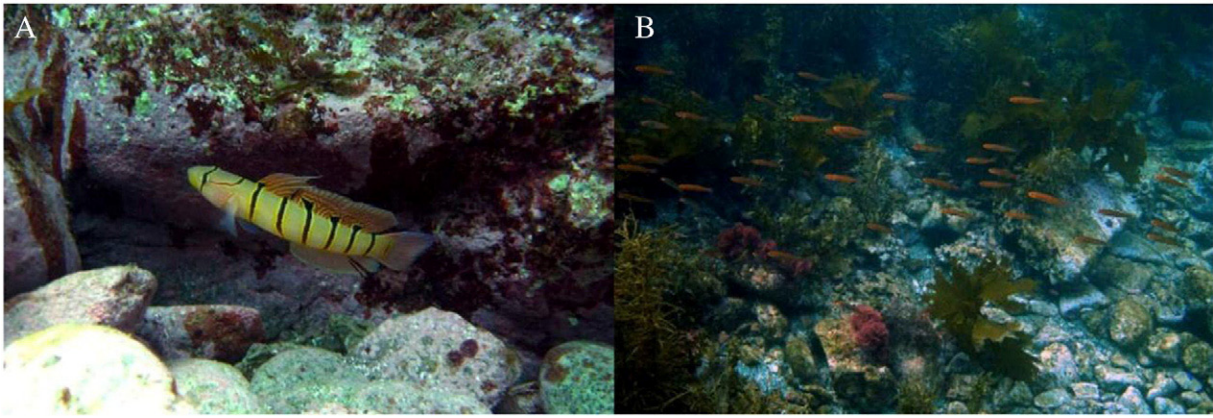
Fig. 3. *Pterogobius elapoides* and *Pterogobius zonoleucus* in their natural habitats. (A) *P. elapoides*, The Sea of Japan, Kyoto Prefecture; (B) *P. zonoleucus*, the Pacific Ocean, Chiba Prefecture.

2.2. DNA amplification and sequencing

We extracted DNA from each of thee 125 samples of *P. elapoides* and *P. zonoleucus*. First, the tissue fragments were incubated overnight at 60 °C in TNES-6M buffer and proteinase K. Then, samples were deproteinized and total DNA was extracted from an individual sample, using the method of Asahida et al. (1996). We designed primers specific to the cytochrome *b* (CytB) and NADH dehydrogenase 2 (ND2) genes that were used for PCR analysis (Akihito et al., 2000).

Polymerase chain reactions (PCRs) were conducted under the following conditions: 1 min at 94 °C, followed by 30 cycles of 30 s each at 94 °C, 30 s at 50 °C, and 1 min at 72 °C, and finally one extra extension step for 5 min at 72 °C. The PCR products were purified using an Ultra Clean PCR Clean-up Kit (MO BIO).

The purified PCR products were sequenced using a cycle-sequencing dye-terminator, called ABI 3730 DNA sequencer. For the CytB and ND2 genes of each sample, sequencing was completed six times for both strands of DNA to ensure the sequence quality. Every effort was made during the entire process of the experiments to avoid mislabeling and contamination.

All sequence data obtained will be deposited in the DDBJ/EMBL/GenBank International DNA sequence data bank under accession numbers AB440348–AB440597.

2.3. Phylogenetic analysis

At first, phylogenetic analyses were carried out on the 125 sequences of the concatenated CytB+ND2+tRNA (Thr, Pro, Trp, Ala) using the maximum likelihood (ML), maximum parsimony (MP) and neighbor-joining (NJ) methods. The ML analysis was performed using the PAUP* ver. 4.0b10 (Swofford, 2001) with the GTR+Γ_4+I model (Rodriguez et al., 1990; Yang, 1996). Prior to the phylogenetic analysis, the MODELTEST (Posada and Crandall, 1998) was used to select the model, and to estimate the shape parameter α of the Γ distribution and I (proportion of invariable sites). By using *P. zacalles* and *P. virgo* as outgroup, the phylogenetic relationships among the samples of *P. elapoides* and *P. zonoleucus* were analyzed. To estimate BPs (Felsenstein, 1985) for the nodes in the tree, 100 replicates were performed. The MP and NJ analyses were performed using PAUP* ver. 4.0b10 (Swofford, 2001) and MEGA3 (Kumar et al., 2004), respectively. For the
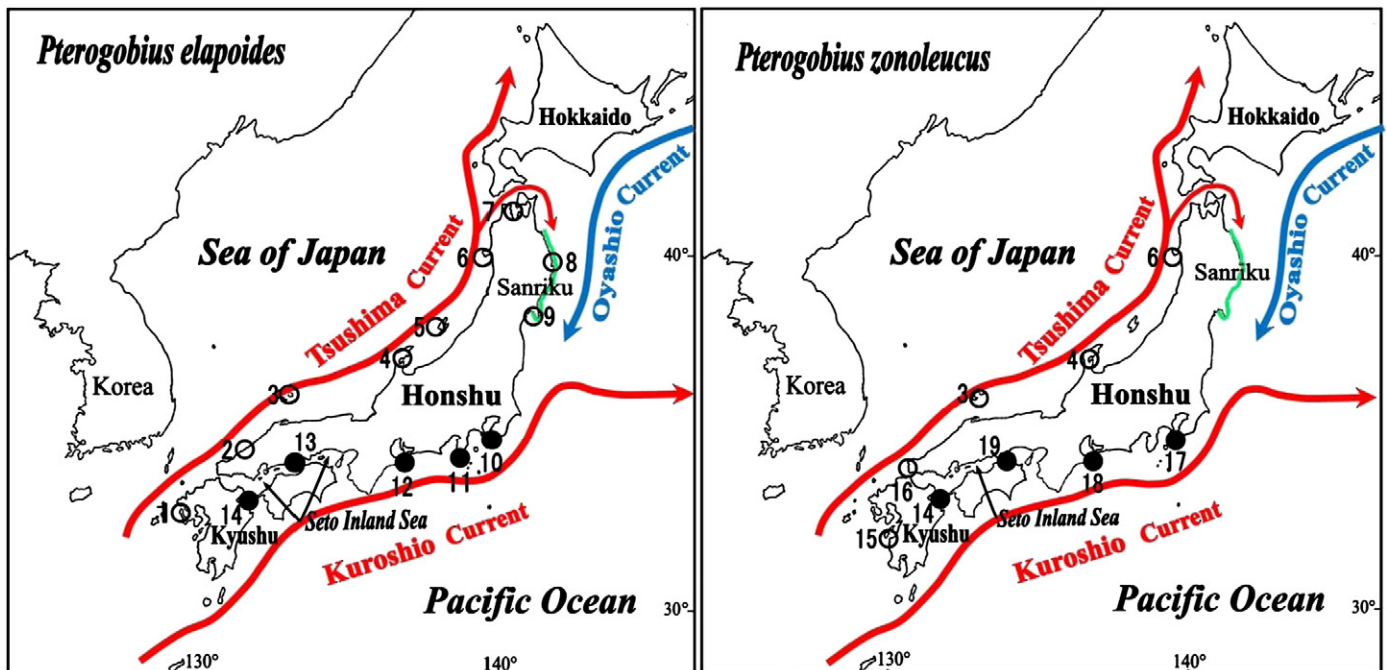

Fig. 4. The sampling localities of *Pterogobius elapoides* and *Pterogobius zonoleucus*: The Sea of Japan population(○), The Pacific Ocean population (●); each number of localities are shown in Table 1. ▉ shows the coast of the Sanriku District; ▉ show the warm currents, ▉ shows the cold current.

Table 1
Data of samples

	Locality (no.)	Sampling date	Specimen number
Pterogobius elapoides			
PeNagasaki 1–5	Sasebo, Nagasaki Pref. (1)	2000/08/18	BLIH 20000276–280
PeShimaneHamada 1–5	Hamada, Shimane Pref. (2)	2000/05/09	BLIH 20000286–290
PeOki 1–5	Oki, , Shimane Pref. (3)	1998/05/01	BLIH 19980161–165
PeIshikawa 1–5	Tsukumo Bay, Ishikawa Pref. (4)	1998/04/04	BLIH 19980166–170
PeSado 1–5	Sado, Niigata Pref. (5)	2000/05/25–26	BLIH 20000271–275
PeAkita 1–5	Oga, Akita Pref. (6)	2000/05/18	BLIH 20000291–295
PeAomori 1–5	Aomori Bay, Aomori Pref. (7)	2000/06/01–07/31	BLIH 20000301–305
PeIwate 1–5	Okirai Bay, Iwate Pref. (8)	1998/08/24	BLIH 19980171–175
PeMiyagi 1–5	Ishinomaki, Miyagi Pref. (9)	2001/09/17	BLIH 20010414–418
PeChiba 1–5	Chikura, Chiba Pref. (10)	2001/05/05–06	BLIH 20010419–423
PeShizuoka 1–5	Shimoda, Shizuoka Pref. (11)	1996/08/17–23	BLIH 19960278–282
PeMie 1–5	Matoya Bay, Mie Pref. (12)	2000/05/25	BLIH 20000296–300
PeHiroshima 1–5	In'noshima, Hiroshima Pref. (13)	2000/05/03–05	BLIH 20000281–285
PeOita 1–5	Saiki Bay, Oita Pref. (14)	1999/10/14	BLIH 19990238–242
P. zonoleucus			
PzoKagoshima 1–5	Nagashima, Kagoshima Pref. (15)	1999/10/18	BLIH 19990208, 229–232
PzoYamaguchi 1–5	Shimonoseki, Yamaguchi Pref. (16)	2004/12/21	BLIH 20040556–560
PzoOki 1–5	Oki, , Shimane Pref. (3)	1998/05/01	BLIH 19980135–139
PzoIshikawa 1–5	Tsukumo Bay, Ishikawa Pref. (4)	1998/04/04	BLIH 19980140–144
PzoAkita 1–5	Oga, Akita Pref. (6)	1998/09/01	BLIH 19980155–159
PzoChiba 1–5	Okinosima, Chiba Pref. (17)	2004/11/16	BLIH 20040561–565
PzoMie 1–5	Gokasho Bay, Mie Pref. (18)	1998/12/07, 09	BLIH 19980145–149
PzoKagawa 1–5	Takamatsu, Kagawa Pref. (19)	1998/09/24	BLIH 19980150–154
PzoOita 1–5	Saiki Bay, Oita Pref. (14)	1999/10/14	BLIH 19990233–237
P. virgo			
PvIshikawa 1	Nanao Bay, Ishikawa Pref.	2003/10/24	BLIH 20030482
PvIshikawa 2	Nanao Bay, Ishikawa Pref.	2003/08/24	BLIH 20030460
PvIshikawa 3	Nanao Bay, Ishikawa Pref.	2003/07/03	NMCI-P 1548
PvIshikawa 4	Nanao Bay, Ishikawa Pref.	2003/08/03	NMCI-P 1564
PvIshikawa 5	Nanao Bay, Ishikawa Pref.	2003/08/07	NMCI-P 1566
P. zacalles			
PzaAomori 1–5	Aomori Bay, Aomori Pref.	1998/06/08–22	BLIH 19980130–134

The numbers in localities of *Pterogobius elapoides* and *P. zonoleucus* which are corresponding with the numbers in Fig. 4.

NJ analysis, the numbers of nucleotide substitutions were estimated by the two-parameter method (Kimura, 1980).

A phylogenetic analysis using the ML method can depend on the assumed model of substitutions, so the assumptions of the models should reflect the real evolutionary process as closely as possible (Hasegawa et al., 1993; Posada and Crandall, 1998). Since the models used in PAUP* are limited, further analyses with a wider variety of models were carried out using PAML ver. 3.13 (Yang, 1997). However,

to overcome limitations in the PAML software, a data set of only 28 sequences was subjected to detailed ML analyses. In the initial ML analysis with PAUP*, no distinction was made between the protein-encoding and tRNA-encoding regions, nor among different codon positions in the protein-encoding genes, but four different models including those which take account of them were applied to this data set. The best model was chosen using the Akaike Information Criterion (AIC) defined by:

$$AIC = -2 \times (\log-likelihood) + 2 \times (number\ of\ parameters).$$

A model that minimizes the AIC is considered to be the most appropriate model in representing the data (Akaike, 1973).

2.4. Morphological characterization

Morphological characters for both species were examined after fixation in 10% formalin and preservation in 70% ethanol. The specimens examined were the same as those subjected to molecular analyses. Measurements were made on 33 morphological characters, including standard length, which generally followed those described by Nakabo (2002) except as noted below. Head depth (depth at the anterior origin of opercle), body depth 1 (depth at the anterior origin of the pelvic fin), body depth 2 (depth at the anterior origin of the second dorsal fin), body width (between the uppermost base of the right and left pectoral fins), predorsal length 1 (from the tip of the snout to the anterior origin of the first dorsal fin), predorsal length 2 (from the tip of the snout to the anterior origin of the second dorsal fin), prepectoral length (from the tip of the snout to the uppermost base of the pectoral fin), prepelvic length (from the tip of the snout to the anterior base of the pelvic fin), caudal-fin length (from the middle point of the caudal-fin base to the posterior-most caudal fin), pelvic fin to anal-fin length (between the anterior base of the pelvic fin and that of the anal-fin), dorso-caudal peduncle length (from the posterior end of the dorsal-fin base to the middle point of the caudal-fin base), ventro-caudal peduncle length (from the posterior end of the anal-fin base to the middle point of the caudal-fin base), and width of second band (width of the second transverse band at the dorsal contour).

Analysis of covariance (ANCOVA) using standard length (SL) as a covariate was used to assess differences in morphometric characters between the Pacific Ocean and the Sea of Japan samples of *P. elapoides* and *P. zonoleucus* respectively, based on our molecular analysis. To provide an objectively defined score that summarizes the major components of variable measurements between the specimens, we conducted a manual principal component analysis (PCA) for each of the two species. Because the length of first dorsal fin differs between males and females (Snyder, 1912), we eliminated these from the statistical analysis and PCA.

Counts were made of the dorsal-fin rays, anal-fin rays, pectoral-fin rays, and transverse bands. The transverse bands were counted as the sum of them on both sides of the body, and when an incomplete band was shown on the caudal peduncle of *P. elapoides* (Fig. 1C), it was counted as "0.5". Mann–Whitney *U*-tests were used to assess differences in counts between the samples of the two species collected from different locations. Furthermore, we noted whether a band from the eyes to the occipital region, which forms a U-shaped marking, was connected in *P. zonoleucus* specimens, because a similar band forms a U-shaped marking in all specimens of *P. elapoides* (Fig. 5A).

3. Results

3.1. Molecular evolutionary analysis

3.1.1. Phylogenetic relationships

The ML tree for the 125 sequences is shown in Fig. 6, in which SJ-*zon*, Pa-*zon*, SJ-*ela*, and Pa-*ela* form monophyletic clades with 100%, 95%, 91%, and 54% BPs respectively, and SJ-*ela* and Pa-*ela* form a
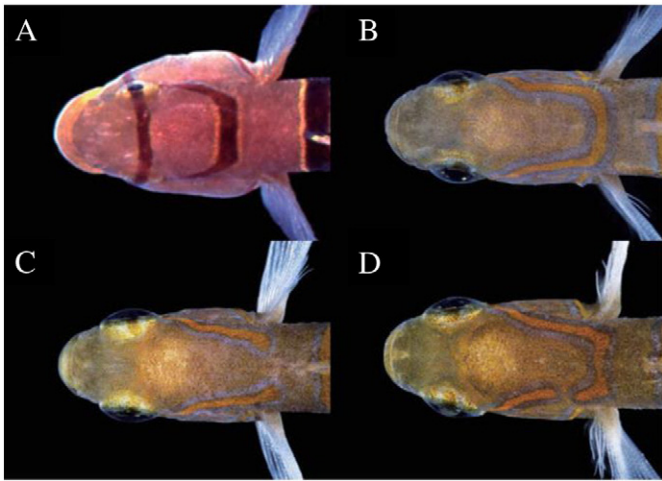
Fig. 5. The marking on the occipital region. (A) *Pterogobius elapoides* (BLIH20030467); (B–D) *Pterogobius zonoleucus*, (B) complete U-shaped marking (BLIH20070463), (C and D) incomplete markings (C: BLIH20070386, D: BLIH20070399).

monophyletic clade with a 99% BP. The former four clades were supported by BPs of 100%, 100%, 98%, and 89% in the MP analysis (Supplementary Fig. S1), and BPs of 100%, 100%, 100%, and 100% in the NJ analysis (Fig. 7). The monophyly of SJ-*ela* and Pa-*ela* was supported by BPs of 100% in the MP and NJ analyses. The Seto Inland Sea population of *P. elapoides* was included in Pa-*ela*. Furthermore, the sequences of *P. zonoleucus* samples do not form a monophyletic clade. Interestingly, SJ-*zon* and the monophyletic *P. elapoides* form a clade excluding Pa-*zon* as an outgroup, and this relationship was supported with a BP of 95% in the ML (Fig. 6), and BPs of 89% and 97% in the MP and NJ analyses (Supplementary Fig. S1 and Fig. 7). The Seto Inland Sea population of *P. zonoleucus* was also included in Pa-*zon*.

Supplementary Fig. S2 shows the tree of the selected 28 sequences estimated using the ML method in PAUP* as well as the MP and NJ methods, and the results are consistent with those of the analysis using all 125 sequences (Fig. 6). The results of the application of the 4 likelihood models described in Supplementary Information to the 28 sequences are shown in Supplementary Table S1. The tree, in which SJ-*zon* and *P. elapoides* form a clade excluding Pa-*zon* as an outgroup, was again consistently supported with BPs in the range of 96.1–98.5% irrespective of the model. From the AIC, the codon-substitution model (Yang, Nielsen and Hasegawa, 1998) for the protein-encoding genes with the partition between the protein-encoding and tRNA-encoding genes best represented the data, but it is remarkable that the phylogenetic relationship was robustly supported irrespective of the model applied; that is, the SJ-*zon*/*P. elapoides* clade was supported with 96.1–98.5% BP and the monophyly of *P. zonoleucus* had BP of only 1.1–3.4%.

In order to check whether the analysis of the 28 sequences was biased by sampling from the 125 sequences, 5 additional datasets were prepared by alternative samplings of 28 sequences. Supplementary Figs. S3-1–5 depict the results of the ML, MP and NJ analyses using PAUP*. The SJ-*zon*/*P. elapoides* clade was supported consistently with BPs of 94–99, 89–96, 96–99%, respectively, in these analyses. Supplementary Table S2 summarizes the results of the ML analyses for the 5 additional datasets (of 28 sequences) using the best available model, and the tree with SJ-*zon*/*P. elapoides* clade was again supported with BP of as high as 96–99%. Therefore, it seems reasonable to assume that the samplings for the 28 sequences well represent the 125 sequences for analyzing the relationships among the Sea of Japan and the Pacific Ocean populations of *P. zonoleucus* and *P. elapoides*.

As a result, we have found that *P. elapoides* is clearly divided into two geographical populations, which almost corresponds to the geographical populations previously described on the basis of
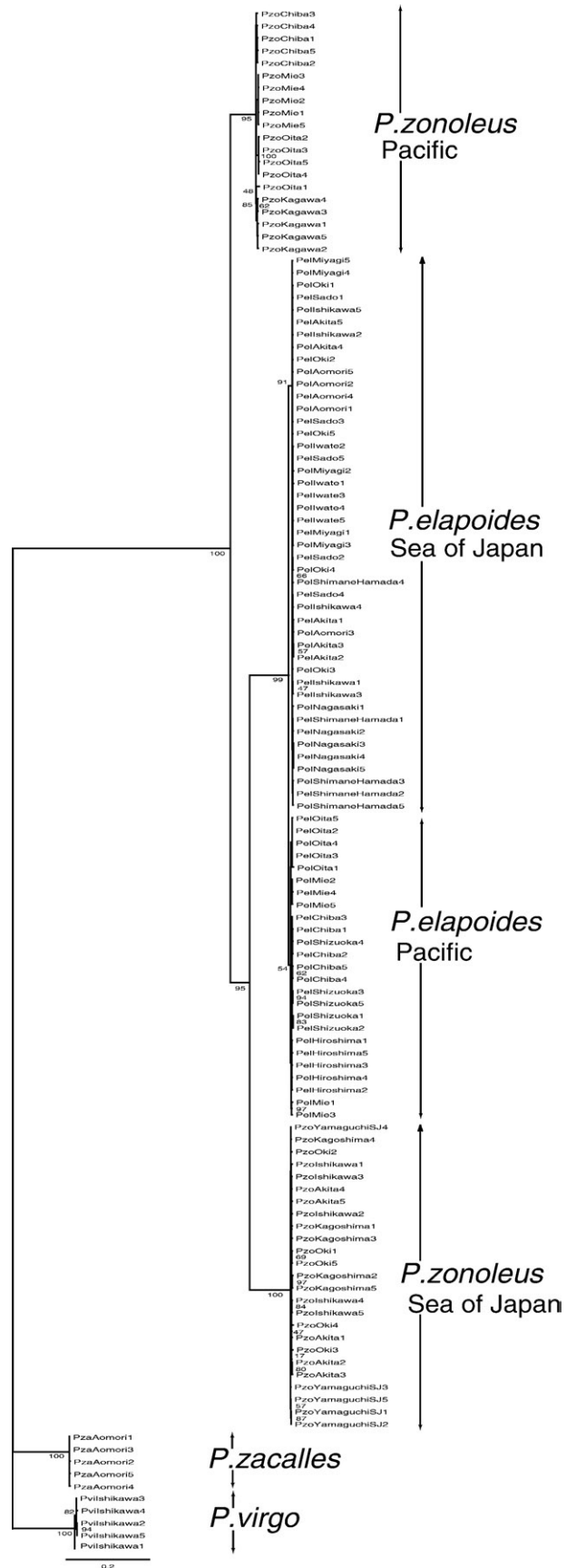
Fig. 6. ML tree of the 125 sequences estimated by PAUP* using the GTR+Γ_4+I model (α=1.64, I=0.57). Branch lengths are proportional to the estimated number of nucleotide substitutions.

Fig. 7. NJ tree of the 125 sequences estimated by MEGA.

Fig. 8. The ML tree of the protein-encoding genes (CytB+ND2) from 110 individuals estimated by the clock model of codon-substitution+Γ_4 (PAML ver.3.13). α=0.86, transition/transversion ratio κ=6.86. Figures at a node represent depth of the node in terms of number of nucleotide substitutions per codon (scale at the bottom) and its SE after ±.

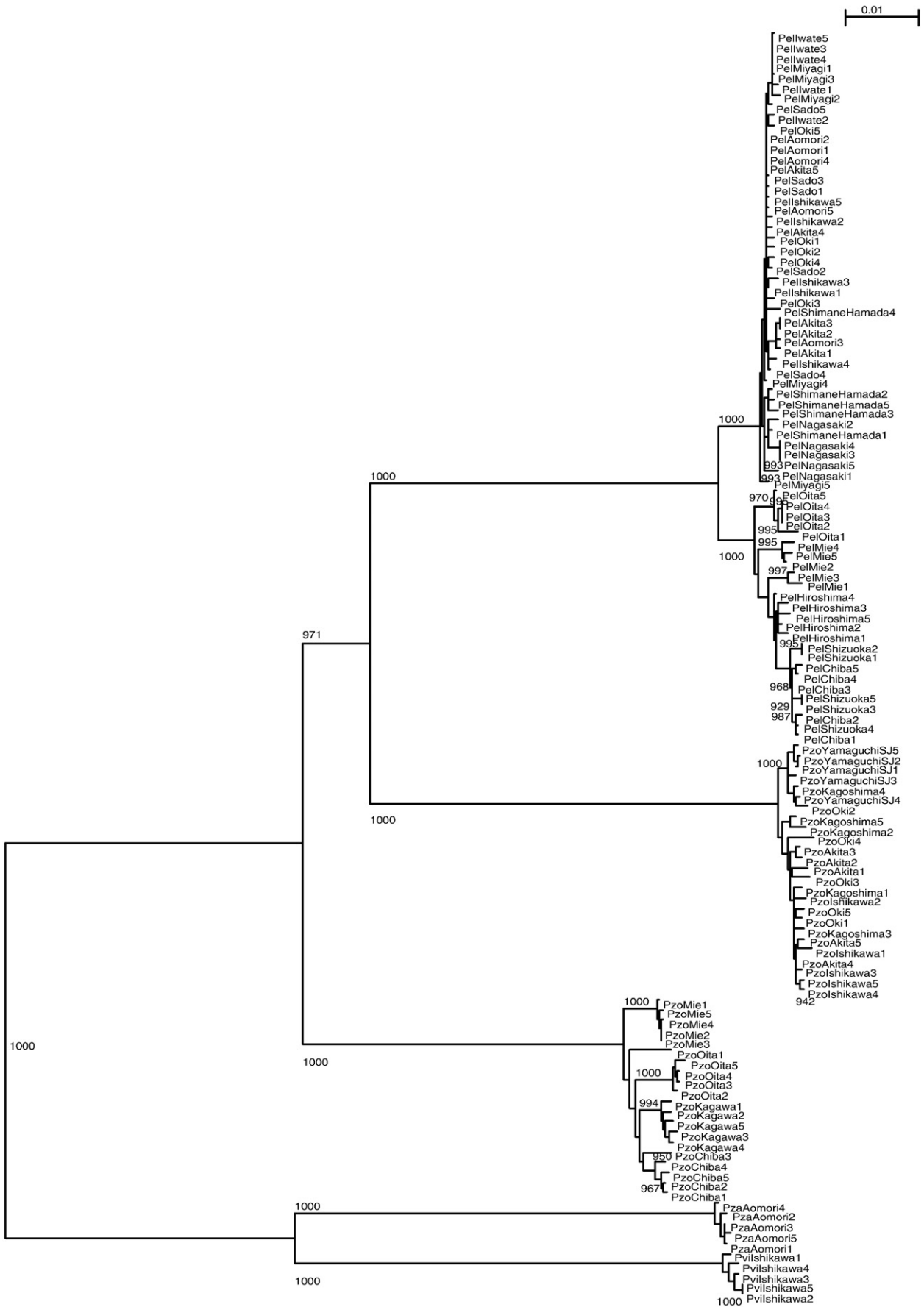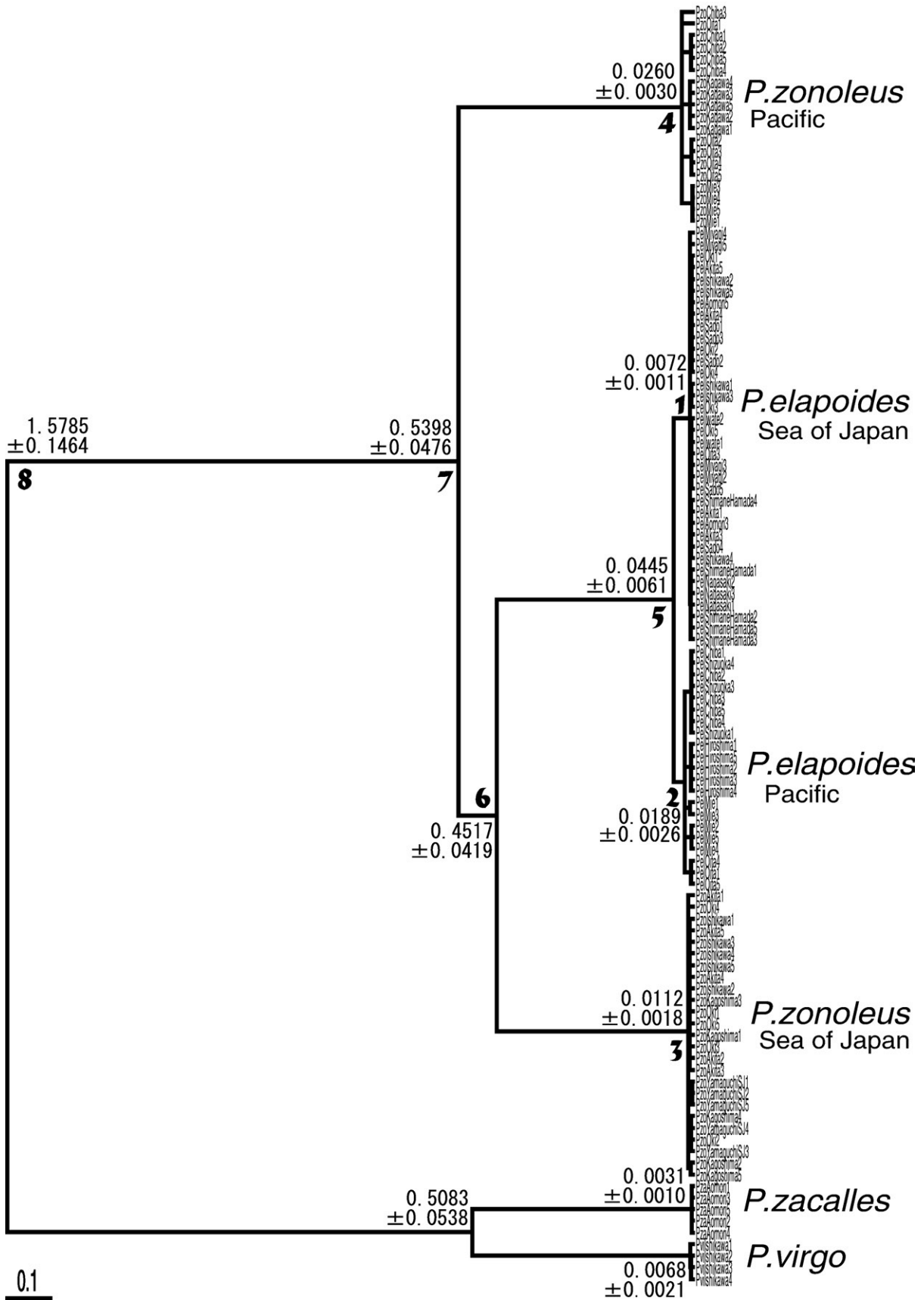morphological characters, except for the Seto Inland Sea population which was formally regarded as an intermediate population. However, we found that these *P. elapoides* populations were derived from one of two groups of *P. zonoleucus* in a constructed molecular phylogeny.

3.1.2. Genetic variation

Our sequence data allow us not only to infer the phylogenetic relationships but also to estimate the relative levels of intra- and inter-specific genetic variation, which is important to obtain a timescale of *Pterogobius* evolution. Fig. 8 shows the ML tree of the protein-encoding genes (CytB+ND2) from 110 individuals estimated with the clock model (the model of constant rates) of codon-substitution+Γ_8 (PAML ver.3.13), using only one individual among those with identical sequences (selected from the 125 individuals). A branch length is proportional to the number of nucleotide substitutions per codon. If the molecular clock holds, relative depth of a node in this figure is proportional to a divergence time.

3.2. Morphological characterization

3.2.1. Pterogobius elapoides

Morphometric characters of Pa-*ela* and SJ-*ela* and the result of the ANCOVA are shown in Table 2. Nine morphometric characters, viz. head length, orbit diameter, predorsal lengths 1 and 2, prepelvic length, preanal-fin length, first dorsal spine length of second dorsal fin, pectoral-fin length, and pelvic fin to anal-fin length, were all significantly different in elevation between the two geographic populations. For example, Pa-*ela* had a significantly larger head, larger eye, longer predorsals (1st dorsal fin and 2nd dorsal fin), and longer prepelvic length than SJ-*ela* at the 1% level of statistical significance. Six characters, head depth, body depth 2, caudal peduncle depth, caudal-fin length, pelvic fin length, and width of the 2nd transverse band, differed in slope between the two populations. For example, the ratio of the width of the 2nd transverse band to standard length decreases with growth in SJ-*ela*, but remains almost constant with growth in Pa-*ela*.

In the PCA, seven morphometric characters, viz. 1st dorsal spine length of 2nd dorsal fin, 2nd dorsal ray length, 3rd dorsal ray length, anal spine length, 1st anal ray length, 2nd anal ray length and caudal-fin length, were not used because the data was lacking for some specimens. The PCA of 22 morphometric characters revealed 92.6% of the total variation expressed in the first two principal components. The greatest contributions to the variance along the first and second axes were made by preanal-fin length (negative) and width of the 2nd transverse band (positive), respectively. Scatter plots of scores on principal components 1 and 2 show separation roughly between the two geographic populations (Fig. 9). Mean PC1 and PC2 scores differed significantly between the two geographic populations (*t*-test, $p < 0.05$ for PC1, $p < 0.01$ for PC2). Although a regression analysis for PC1 against the standard length was significant, that for PC2 was not ($p = 0.90$), indicating the size effect had been removed from the scores on PC2. Mean PC3 scores were not significantly different between the two geographic populations.

The numbers of dorsal-fin, anal-fin and pectoral-fin rays are given in Table 3. The number of dorsal-fin rays was 20–23 (mode 21) in Pa-*ela* and 19–22 (mode 20) in SJ-*ela*, and were significantly different between two populations (Mann–Whitney *U*-test, $p < 0.05$). That of anal-fin rays was 19–22 (mode 20) in the former and 18–22 (mode 20) in the latter, was also significantly different ($p < 0.01$). In addition, the number of pectoral-fin rays was 21–24 (mode 22) in Pa-*ela* and 19–22 (mode 21) in SJ-*ela*. The difference in the number of pectoral-fin rays between the two geographic populations was significant ($p < 0.01$).

Table 2
Measurements of *Pterogobius elapoides* and *P. zonoleucus*, and the significance differences in elevations by ANCOVA between the Pacific and Sea of Japan populations in each species

	Pterogobius elapoides			*Pterogobius zonoleucus*		
	Pacific population	Sea of Japan population	Significance	Pacific population	Sea of Japan population	Significance
Standard length (SL)	43.74–78.61 mm	38.54–71.96 mm		38.04–52.84 mm	38.17–64.58 mm	
In % SL						
Head length	29.1 (27.1–31.3, 25)	28.1 (26.1–29.4, 45)	**	27.5 (26.1–28.3, 20)	26.4 (24.5–27.7, 25)	*
Head depth	15.9 (14.2–17.6, 25)	6.1 (14.2–19.8, 45)	(*)	15.5 (13.8–16.8, 20)	16.4 (15.5–18.5, 25)	**
Snout length	8.3 (7.5–10.0, 25)	8.0 (6.7–9.5, 45)	ns	6.4 (5.7–7.2, 20)	6.1 (4.9–7.0, 25)	*
Orbit diameter	7.0 (5.9–8.8, 25)	6.3 (5.3–7.4, 45)	**	8.3 (6.9–9.0, 20)	7.6 (6.4–8.5, 25)	ns
Interorbital width	7.5 (5.9–9.0, 25)	7.9 (6.7–9.3, 45)	ns	7.1 (5.4–8.5, 20)	7.3 (5.4–8.1, 25)	(**)
Body depth 1	16.7 (14.2–18.7, 25)	16.6 (14.1–21.0, 45)	ns	16.5 (14.8–18.5, 20)	17.1 (15.1–19.2, 25)	*
Body depth 2	18.1 (15.9–21.1, 25)	17.8 (14.4–22.1, 45)	(*)	18.1 (16.0–20.6, 20)	18.1 (14.2–21.9, 25)	ns
Body width	11.8 (10.3–13.4, 25)	11.0 (8.8–13.5, 45)	ns	11.0 (9.7–12.8, 20)	11.3 (9.5–13.7, 25)	*
Caudal peduncle depth	10.4 (9.4–11.7, 25)	9.8 (7.7–12.3, 45)	(*)	10.7 (9.7–11.6, 20)	10.0 (8.8–11.6, 25)	*
Upper jaw length	10.4 (8.8–11.9, 25)	10.3 (8.9–12.6, 45)	ns	9.8 (8.7–11.7, 20)	10.1 (9.1–11.0, 25)	(**)
Predorsal length 1	35.1 (33.2–37.4, 25)	34.2 (32.1–36.6, 45)	**	34.2 (32.5–36.1, 20)	33.3 (31.2, 35.3, 25)	ns
Predorsal length 2	53.9 (52.1–56.3, 25)	53.0 (49.3–56.5, 45)	**	53.3 (51.3–55.7, 20)	52.7 (55.6–60.4, 25)	ns
Prepelvic length	29.0 (24.5–31.2, 25)	27.7 (24.9–30.5, 45)	**	28.4 (25.5–32.9, 20)	27.9 (25.8–30.2, 25)	ns
Preanal-fin length	57.6 (54.3–60.3, 25)	56.4 (53.0–59.0, 45)	*	57.9 (56.2–59.6, 20)	57.7 (55.6–60.4, 25)	ns
Prepectoral length	30.0 (18.8–32.6, 25)	29.4 (26.8–31.2, 45)	ns	29.6 (28.0–30.7, 20)	28.1 (26.2–30.3, 25)	**
1st dorsal spine length (1st dorsal fin)	12.6 (10.2–15.1, 25)	12.9 (10.3–18.1, 45)	–	12.6 (10.4–13.5, 20)	13.2 (11.0–16.9, 25)	–
2nd dorsal spine length (1st dorsal fin)	16.8 (12.5–25.9, 24)	15.7 (11.3–26.6, 45)	–	17.4 (14.8–23.2, 20)	18.8 (12.8–24.7, 25)	–
3rd dorsal spine length (1st dorsal fin)	22.5 (12.9–36.9, 25)	19.6 (13.0–44.9, 45)	–	21.7 (17.7–29.5, 20)	24.9 (16.0–39.7, 25)	–
1st dorsal spine length (2nd dorsal fin)	10.4 (9.3–12.0, 25)	9.7 (7.8–13.5, 45)	*	10.2 (8.1–12.0, 20)	9.9 (6.6–11.5, 24)	ns
1st dorsal ray length	12.4 (10.9–13.7, 25)	12.4 (9.8–14.1, 44)	ns	12.3 (10.9–14.1, 20)	12.1 (10.3–13.4, 25)	ns
2nd dorsal ray length	13.3 (11.4–14.6, 25)	13.6 (11.7–16.4, 45)	ns	13.9 (12.5–16.2, 20)	13.2 (11.0–15.1, 25)	ns
3rd dorsal ray length	13.8 (12.4–15.2, 24)	13.6 (12.0–16.4, 45)	ns	14.4 (13.4–16.2, 20)	13.8 (12.0–15.8, 25)	ns
Anal spine length	6.5 (5.5–7.5, 24)	6.6 (5.3–8.0, 44)	ns	6.5 (5.1–7.3, 20)	6.1 (5.0–8.7, 24)	ns
1st anal ray length	9.4 (8.1–11.4, 24)	9.7 (6.5–11.8, 45)	ns	8.9 (6.3–10.1, 20)	8.4 (6.8–11.5, 25)	ns
2nd anal ray length	11.6 (10.2–13.8, 24)	11.7 (8.5–15.0, 44)	ns	11.0 (8.9–12.9, 20)	10.7 (9.3–13.3, 25)	(*)
Caudal-fin length	24.0 (14.8–27.6, 23)	23.7 (20.6–32.9, 42)	(*)	22.9 (20.6–24.1, 19)	22.5 (20.4–26.4, 24)	ns
Pectoral-fin length	23.7 (20.4–27.3, 25)	22.5 (18.2–25.9, 45)	*	24.0 (20.9–26.0, 20)	23.2 (20.6–26.4, 25)	*
Pelvic fin length	15.4 (13.7–17.8, 25)	14.6 (12.4–18.2, 45)	(**)	15.6 (13.8–17.4, 20)	16.1 (13.3–18.1, 25)	ns
Pelvic fin to anal anal-fin length	28.8 (24.6–31.8, 25)	29.1 (24.9–32.9, 45)	*	29.9 (26.4–31,7, 20)	31.0 (27.2–33.7, 25)	(*)
Dorso-peduncle length	13.4 (11.8–14.4, 25)	13.9 (11.4–16.3, 45)	ns	16.0 (14.8–17.7, 20)	15.6 (14.3–17.6, 25)	ns
Ventro-peduncle length	15.0 (12.7–16.7, 25)	15.5 (13.8–17.8, 45)	ns	16.6 (15.1–17.9, 20)	16.0 (13.8–17.9, 25)	ns
Width of 2nd transverse band	3.3 (2.4–4.3, 25)	2.4 (1.4–3.9, 45)	(**)	–	–	–

*: $p < 0.05$, **$p < 0.01$, ns: not significant. Difference in slopes indicated in parenthesis.
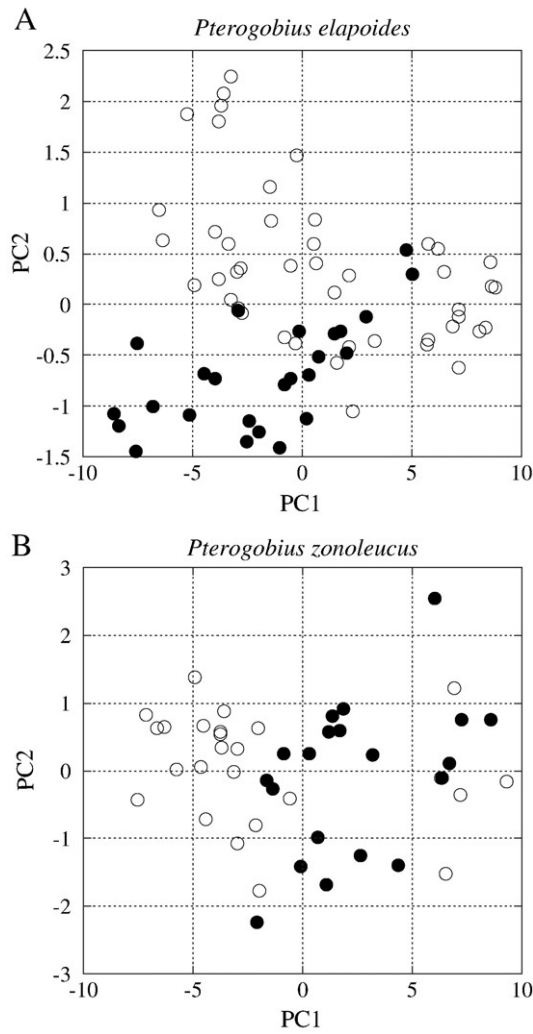
Fig. 9. Plots of the first two principal components scores based on the morphometric characters of *Pterogobius elapoides* (A) and *P. zonoleucus* (B). Open circles: Sea of Japan population. Solid circles: Pacific population.

Table 4
Counts of transverse dark bands in *Pterogobius elapoides* and *P. zonoleucus*

	Transverse dark bands				
	10	11	12	13	14
Pterogobius elapoides					
Pacific population					
Kamiura, Oita Pref.	–	–	5	–	–
In'noshima, Hiroshima Pref.	–	–	–	5	–
Nanzei, Mie Pref.	–	–	5	–	–
Shimoda, Shizuoka Pref.	–	–	5	–	–
Awa, Chiba Pref.	–	–	5	–	–
Sea of Japan population					
Sasebo, Nagasaki Pref.	–	–	–	–	5
Hamada, Shimane Pref.	–	–	–	–	5
Oki, Shimane Pref.	–	–	–	–	5
Noto, Ishikawa Pref.	–	–	–	–	5
Sado, Niigata Pref.	–	–	–	–	5
Oga, Akita Pref.	–	–	–	–	5
Kita-tsugaru, Aomori Pref.	–	–	–	4	1
Sanriku, Iwate Pref.	–	–	–	2	3
Ishinomaki, Miyagi Pref.	–	–	–	4	1
Pterogobius zonoleucus					
Pacific population					
Kamiura, Oita Pref.	1	1	3	–	–
Takamatsu, Kagawa Pref.	–	–	2	–	–
Nanzei, Mie Pref.	–	–	3	–	–
Tateyama, Chiba Pref.	2	–	1	–	–
Sea of Japan population					
Izumi, Kagoshima Pref.	5	–	–	–	–
Shimonoseki, Yamaguchi Pref.	3	–	2	–	–
Oki, Shimane Pref.	2	2	1	–	–
Noto, Ishikawa Pref.	5	–	–	–	–
Oga, Akita Pref.	2	–	1	–	–

bands on each side of the body is 6.5 (13 in total) in the five specimens from Hiroshima Prefecture in Pa-*ela* and in the ten specimens from Aomori, Iwate and Miyagi Prefectures in SJ-*ela* (Table 4).

The dark band from the eye to the occipital region formed a complete U-shape marking uniformly in the two geographic populations (Fig. 5A).

3.2.2. Pterogobius zonoleucus

Morphometric characters of the two geographic populations and the results of the ANCOVA are shown in Table 2. The width of the second band was not measured, since it was indistinct in some specimens. Six morphometric characters, viz. head length, snout length, body depth 1, body width, caudal peduncle depth and pectoral-fin length, were significantly different in elevation between the two populations at the 5% level, and two characters, viz. head depth and prepectoral length, were significantly different at the 1% level. Among these, plots of head depth, body width, and body depth 1 respectively in standard length almost separated the two geographic populations. In slopes, four characters, viz. interorbital width, upper jaw length, 2nd anal ray length, pelvic to anal-fin length, were different between the two geographic populations.

The number of transverse dark bands on the body in each geographic population is shown in Table 4. The number of transverse dark bands on the body was usually six on each side (12 in total) in Pa-*ela*, but was usually seven on each side (14 in total) in SJ-*ela*. The difference in the number of transverse dark bands on the body between the two geographic populations was significant (Mann–Whitney *U*-test, $p < 0.01$).

As stated above, significant morphological differences between the two geographic populations were evident for some morphometric characters: the number of dorsal-fin rays, anal-fin rays, pectoral-fin rays and transverse dark bands. However, the number of transverse

Table 3
Counts of *Pterogobius elapoides* and *P. zonoleucus*

	Dorsal-fin rays						Anal-fin rays						Pectoral-fin rays					
	18	19	20	21	22	23	17	18	19	20	21	22	19	20	21	22	23	24
Pterogobius elapoides																		
Pacific population	–	–	8	14	2	1	–	–	4	12	8	1	–	–	4	11	9	1
Sea of Japan population	–	6	20	16	3	–	–	6	14	18	6	1	1	12	16	13	3	–
Pterogobius zonoleucus																		
Pacific population	–	4	14	2	–	–	1	4	9	6	–	–	–	3	6	9	2	–
Sea of Japan population	1	5	12	7	–	–	1	5	8	10	1	–	–	1	8	12	4	–

In the PCA, three morphometric characters, viz. 1st dorsal spine length of 2nd dorsal fin, anal spine length and caudal-fin length, were not used because of a lack of data for some specimens. The PCA of the other 26 morphometric characters revealed 87.1% of the total variation expressed in the first two principal components. The greatest contributions to the variance along the first and second axes were made by standard length (positive) and 1st anal-fin ray length (negative), respectively. Scatter plots of scores for principal component (PC) 1 of Pa-*zon* roughly separated it from that of SJ-*zon*, but which was largely factored by size effect (Fig. 9). In fact, regression between the standard length and PC1 scores was statistically significant ($p < 0.01$). On the other hand, mean scores of PC2 were not significantly different between the two geographic populations. The regression for PC2 was not significant ($p = 0.637$), indicating that size effects had been removed.

Countable characters are shown in Table 3. The number of dorsal-fin rays was 19–21 (mode 20) in Pa-*zon* and 18–21 (mode 20) in SJ-*zon*, that of anal-fin rays was 17–20 (mode 19) in the former and 17–21 (mode 20) in the latter, and that of pectoral-fin rays was 20–23 (mode 22) both in the two geographic populations. The numbers of these fin rays were not significantly different between the two geographic populations.

The number of transverse light bands on the body in Pa-*zon* was modally 6 (a total of 12 on both sides), but in SJ-*zon* was modally 5 (a total of 10 on both sides). Pa-*zon* differed significantly from SJ-*zon* in the number of transverse dark bands, according to a Mann–Whitney *U*-test. Further, the number of transverse bands on both sides varied between specimens collected from different localities: among the Pa-*zon* samples, three specimens from Oita and Chiba Prefectures had five on either side of the body 5 (10 in total), and one specimen from Oita Prefecture had 5 five on one side of the body and 6 on the other (11 in total); for SJ-*zon* samples, two specimens from Shimane Prefecture had 5 on one side of the body and 6 on the other (11 in total), and four specimens from Yamaguchi, Shimane and Akita Prefectures had 6 on both sides of the body (12 in total).

The light band from the eye to the occipital region (Fig. 5B–D) was usually connected with that on the other side to form a complete U-shaped marking in 55% of the specimens of Pa-*zon*, but only in 16% of the specimens of SJ-*zon*.

4. Discussion

4.1. Molecular level

In general, phylogenetic inference based on the ML results depends on the assumptions of the model (e.g., Nikaido et al., 2003; Takishita et al., 2005), so use of the best available model is recommended. However, if the inferred tree varies among different models, we cannot put a large reliance on the tree inferred from the best model, because even that model is merely a rough approximation of the real evolutionary process and further improvement of the model might change the result. Therefore, strong support for a particular tree irrespective of the model, as in our case, is a good indicator of the reliability of the inferred tree. The congruent results by the MP and NJ analyses further reinforce our conclusion that SJ-*zon* and Pa-*zon* do not form a monophyletic clade and that the former population is phylogenetically closer to *P. elapoides* than to the latter population.

The evolutionary relationships among a total of four geographic populations for *P. elapoides* and *P. zonoleucus* require robust explanations. In particular, we cannot help considering the possibility that SJ-*zon* should be treated as a separate species from Pa-*zon* because SJ-*zon* is evolutionarily much closer to the two geographic populations of *P. elapoides* than Pa-*zon*. Interestingly, Ma et al. (2006) have observed a very similar feature in two types of two species of the Asian common minnow, *Zacco pachycephalus* and *Z. platypus*.

Although they have analyzed genomic DNA by AFLPs (Amplified fragment length polymorphisms), they showed that after type L1 of *Z. platypus* separated from type L2 of the same species, the two types of *Z. pachycephalus* (A1 and A2) separated from the ancestor of type L1 of *Z. platypus*. In their study, Ma and colleagues proposed that these four different types be redefined as four independent species. A similar situation has also been observed in mitochondrial DNA variations in other species such as brown bears (*Ursus arctos*) and polar bears (*Ursus maritimus*) (Shields et al., 2000). In particular, brown bears of Admiralty Island, Baranof Island, and Chichagof Island of southeastern Alaska showed a phylogenetically closer relationship to polar bears in Canada, Hudson Bay and Siberia than two brown bears in Southeast Alaska mainland and Kenai Peninsula. Although this special group of brown bears has not been given a new species name, a satisfactory evolutionary explanation remains to be given.

4.2. Genetic distances

The depth of the last common ancestor (LCA) of SJ-*ela* and Pa-*ela* (node 5 in Fig. 8) in terms of the number of nucleotide substitutions per codon is 0.0445 ± 0.0061 (± refers to 1 SE), while the depth of the LCA of Pa-*zon* and SJ-*zon*/all the *P. elapoides* (node 7) is 0.5398 ± 0.0476. The intra-specific genetic variation among *P. zonoleucus* is thus much larger than that among *P. elapoides* by 12.12 ± 1.98 times. If the molecular clock holds, this ratio is equal to the ratio of the divergence times.

As for intra-population genetic diversity, the depths of the LCAs for Pa-*ela* and Pa-*zon* are 0.0189 ± 0.0026 and 0.0260 ± 0.0030, respectively, whereas those of SJ-*ela* and SJ-*zon* are 0.0072 ± 0.0011 and 0.0112 ± 0.0018. For both *P. elapoides* and *P. zonoleucus*, the genetic diversities of the Pacific populations are larger than those of the Sea of Japan by 2.65 ± 0.53 and 2.31 ± 0.46 times, respectively.

We now speculate on how the differences in genetic diversity between the Pacific Ocean and the Sea of Japan populations are related to their ecological situations for both *P. elapoides* and *P. zonoleucus*. During the last glacial age, the Tsushima Current, a branch of the warm Kuroshio Current at present, did not flow into the Sea of Japan. The modern oceanographic regime was established in the Sea of Japan about 8 ka (8000 years ago) after the opening of the Tsushima Strait between Kyushu and Korea that allowed an inflow of the warm Tsushima Current (Oba et al., 1991). Since the depth of the LCA of SJ-*ela* and that of SJ-*zon* do not differ very much and are much younger than those of the Pacific populations of the two species, the diversification of each of the former two populations might have been caused by this common environmental factor. We tentatively assumed that the diversification of the Sea of Japan populations was caused by the opening of the Tsushima Strait and that the date of node 1 or node 3 was 8 ka when calibrating the molecular clock (Table 5). Then, the

Table 5
Genetic distances relative to node 1 or 3 in Fig. 8

		Relative genetic distance[a]	Divergence time (ka)[b]
SJ-*ela*	Node 1	1	8
SJ-*zon*	Node 3	1	8
Pa-*ela*/SJ-*ela*	Node 2/node 1	2.65 ± 0.53	21 ± 4
Pa-*zon*/SJ-*zon*	Node 4/node 3	2.31 ± 0.46	18 ± 4
(SJ-*ela* vs Pa-*ela*)/SJ-*ela*	Node 5/node 1	6.23 ± 1.26	50 ± 10
(SJ-*ela* vs Pa-*ela*)/SJ-*zon*	Node 5/node 3	3.97 ± 0.84	32 ± 7
(*P.ela* vs SJ-*zon*)/SJ-*ela*	Node 6/node 1	63.17 ± 11.05	505 ± 88
(*P.ela* vs SJ-*zon*)/SJ-*zon*	Node 6/node 3	40.25 ± 7.46	322 ± 60
(Pa-*zon* vs SJ-*zon*)/SJ-*ela*	Node 7/node 1	75.49 ± 13.02	604 ± 104
(Pa-*zon* vs SJ-*zon*)/SJ-*zon*	Node 7/node 3	48.11 ± 8.81	385 ± 71

Numberings of the nodes are for Fig. 8.
[a] Genetic distances are from Fig. 8, and a figure after ± is 1 SE.
[b] Divergence time estimated by assuming diversification of "the Sea of Japan *P. elapoides*" (node 1) or that of "the Sea of Japan *P. zonoleucus*" (node 3) occurred 8 ka (thousand years ago).

divergence time between the Sea of Japan and the Pacific populations of *P. elapoides* (node 5) was estimated to be 50±10 or 32±7 ka, depending on whether node 1 or node 3 was used in calibrating the clock. On the other hand, the divergence between *P. elapoides* and SJ-*zon* (node 6) was estimated to be 505±88 or 322±60 ka, and the divergence between the Sea of Japan and the Pacific populations of *P. zonoleucus* (node 7) was estimated to be 604±104 or 385±71 ka. We could thus obtain a tentative timeline for the evolution of *P. elapoides* and *P. zonoleucus*, but the evolutionary and paleoenvironmental implications of these estimates remain to be elucidated.

4.3. Geographical distribution and currents

Distributions of the two geographic populations of both *P. elapoides* and *P. zonoleucus* seem to correspond roughly to the routes of the warm Tsushima and Kuroshio Currents and the cold Oyashio Current. Jordan and Snyder (1901) noted a difference in the geographical distribution of *P. daimio*, which is found in the south, and *P. elapoides*, which is found farther north. According to this study, SJ-*ela* which corresponds to the *P. elapoides* of Jordan and Snyder (1901) is distributed from the Sea of Japan coast of northwestern Kyushu northward to southwestern Hokkaido and the Sanriku District, whereas Pa-*ela* which corresponds to the *P. daimio* of Jordan and Snyder (1901) is distributed along the Pacific coast of central Honshu, throughout the Seto Inland Sea, and along the eastern coast of Kyushu. The former is distributed in the Tsushima Current area, and the latter is distributed in the Kuroshio Current area, which is warmer than the Tsushima Current area.

SJ-*zon* is distributed from the Sea of Japan coast of western Kyushu northward to the northwestern coast of Honshu and southwestern Hokkaido (T. Taguchi personal communication), but does not reach the Sanriku District which is colder than these areas; Pa-*zon* is distributed along the Pacific coast of central Honshu, throughout the Seto Inland Sea, and along the eastern coast of Kyushu. As mentioned above, *P. zonoleucus* has a distribution similar to that of *P. elapoides* except for the Sanriku District, which is affected by the cold Oyashio Current. In early spring, the range of the water temperature in each area of shallow coast at 10 m depth in the Sanriku District was 4.5–6.6 °C (the average water temperature) and −0.4–2.2 °C (the lowest water temperature), whereas it was 7.9–15.7 °C and 4.4–12.9 °C respectively along the Tsushima Current coast from northwestern Kyushu northward to northwestern Honshu (the mean water temperature in March from 1906–2003, Japan Oceanographic Data Center). Therefore *P. zonoleucus* seems less tolerant of cold water than *P. elapoides*.

Similar geographic distributions for two intra-specific populations around the Japanese Archipelago is also found in *Ditrema temminckii*, Japanese surfperch (Katafuchi and Nakabo, 2007), *Turbo (Batillus) cornutus*, Japanese turban shell (Kojima et al., 1997, 2000) and *Batillaria cumingi*, the direct-developing intertidal gastropod (Kojima et al., 2004).

4.4. Morphological level

Although the genetic distance was much shorter between Pa-*ela* and SJ-*ela* than between Pa-*zon* and SJ-*zon*, the differences in color pattern (Table 4), morphometric characters (Fig. 9A and B), and counts of fin rays (Table 3) were more evident in the former than in the latter. The differences in morphometric characters were evident between Pa-*ela* and SJ-*ela* and between Pa-*zon* and SJ-*zon*, but more significant differences were found in the former (nine characters differed significantly) than the latter (six characters differed significantly).

Although the two geographical populations of *P. elapoides* mostly differed in the number of transverse dark bands on the body as described previously, there were some intermediate variations between these two. Some specimens from Hiroshima Prefecture among Pa-*ela* had a dark incomplete band instead of a dark band on the caudal peduncle and fewer pectoral-fin rays compared to other specimens of Pa-*ela*. Among SJ-*ela*, some specimens from Aomori, Iwate and Miyagi Prefectures had a dark incomplete band like the specimens from Hiroshima Prefecture and more pectoral-fin rays than other specimens of SJ-*ela*. They were clearly separated from each other based on the molecular data. Accordingly, these intermediate individuals may not be caused by hybridization.

The two geographical populations of *P. zonoleucus* differed in the number of transverse light bands on the body; however, the difference was not as clear as the difference in the number of the transverse dark bands in the two geographical populations of *P. elapoides*. The band from the eyes to the occipital region differed in the percentage of a complete U-shaped marking in the two geographical populations of *P. zonoleucus*, whereas all the specimens of the two geographical populations of *P. elapoides* had a complete U-shaped marking. The morphological differences of the two geographical populations of *P. zonoleucus* were first found in the present work.

In conclusion, we discussed the evolutionary relationships among SJ-*ela*, Pa-*ela*, SJ-*zon*, and Pa-*zon* based on the phylogenetic relationship determined by our molecular analysis, and compared those with the morphological differences among these four geographical populations. We recognized *P. virgo* and *P. zacalles* as outgroups of these four clades. We found not only the morphological difference but also the molecular difference in the two geographical populations of *P. elapoides* and *P. zonoleucus*. We found that the degree of morphological difference was not in accordance with the molecular difference seen in the two geographic populations of *P. elapoides* and *P. zonoleucus*. This obvious discrepancy between morphological and molecular features was discussed from the evolutionary point of view.

Appendix A. Supplementary data

Supplementary data associated with this article can be found, in the online version, at doi:10.1016/j.gene.2008.09.026.

References

Akaike, H., 1973. Information theory and an extension of the maximum likelihood principle. In: Petrov, B.N., Csaki, F. (Eds.), Second International Symposium on Information Theory. Akademiai Kiado, Budapest, pp. 267–281.

Akihito, P., 1984. *Pterogobius elapoides*. In: Masuda, H., Amaoka, K., Araga, C., Uyeno, T., Yoshino, T. (Eds.), The Fishes of the Japanese Archipelago. Tokai University Press, Tokyo, pp. 279–280. 254B, C.

Akihito, Iwata, A., Kobayashi, T., Ikeo, K., Imanishi, T., Ono, H., Umehara, Y., Hamamatsu, C., Sugiyama, K., Ikeda, Y., Sakamoto, K., Fumihito, A., Ohno, S., Gojobori, T., 2000. Evolutionary aspects of gobioid fishes based upon a phylogenetic analysis of mitochondrial cytochrome *b* genes. Gene 259, 5–15.

Asahida, T., Kobayashi, T., Saitoh, K., Nakayama, I., 1996. Tissue preservation and total DNA extraction from fish stored at ambient temperature using buffers containing high concentration of urea. Fish. Sci. 62 (5), 727–730.

Felsenstein, J., 1985. Confidence limits on phylogenies: an approach using the bootstrap. Evolution 39, 783–791.

Günther, A., 1871. Report on several collections of fishes recently obtained for the British. Museum. Proc. Zool. Soc. Lond. 652–675, 53–70.

Hasegawa, M., Hashimoto, T., Adachi, J., Iwabe, N., Miyata, T., 1993. Early branchings in the evolution of eukaryotes: ancient divergence of *Entamoeba* that lacks mitochondria revealed by protein sequence data. J. Mol. Evol. 36, 380–388.

Jordan, D.S., Snyder, J.O., 1901. A review of the gobioid fishes of Japan, with descriptions of twenty-one new species. Proc. U. S. Natl. Mus. 24 (1244), 33–132.

Katafuchi, H., Nakabo, T., 2007. Revision of the East Asian genus *Ditrema* (Embiotocidae), with description of a new subspecies. Ichthyol. Res. 54, 350–366.

Kimura, M., 1980. A simple method for estimating evolutionary rates of base substitutions through comparative studies of nucleotide sequences. J. Mol. Evol. 16 (2), 111–120.

Kojima, S., Sagawa, S., Hayashi, I., 1997. Genetic differentiation among populations of the Japanese turban shell *Turbo* (*Batillus*) *cornutus* corresponding to warm currents. Mar. Ecol., Prog. Ser. 150, 149–155.

Kojima, S., Sagawa, R., Hayashi, I., 2000. Stability of the courses of the warm coastal currents along the Kyushu Island suggested by the population structure of the Japanese turban shell, *Turbo* (*Batillus*) *cornutus*. J. Oceanogr. 56, 601–604.

Kojima, S., Hayashi, I., Kim, D., Iijima, A., Furota, T., 2004. Phylogeography of an intertidal direct-developing gastropod *Batillaria cumingi* around the Japanese islands. Mar. Ecol., Prog. Ser. 276, 161–172.

Kumar, S., Tamura, K., Nei, M., 2004. MEGA3: integrated software for molecular evolutionary genetics analysis and sequence alignment. Brief Bioinform. 5 (2), 150–163.

Ma, G.-C., Tsao, H.-S., Lu, H.-P., Yu, H.-T., 2006. AFLPs congruent with morphological differentiation of Asian common minnow *Zacco* (Pisces: Cyprinidae) in Taiwan. Zool. Scr. 35 (4), 341–351.

Nakabo, T., 2002. Introduction to ichthyology, In: Nakabo, T. (Ed.), Fishes of Japan with Pictorial Keys to the Species, English edition. Tokai University Press, Tokyo, pp. xxi–xlii.

Nikaido, M., Cao, Y., Harada, M., Okada, N., Hasegawa, M., 2003. Mitochondrial phylogeny of hedgehogs and monophyly of Eulipotyphla. Mol. Phylogenet. Evol. 28 (2), 276–284.

Oba, T., Kato, M., Kitazato, H., Koizumi, I., Omura, A., Sakai, T., Takayama, T., 1991. Palaeoenvironmental changes in the Japan Sea during the last 85,000 years. Palaeoceanography 6, 499–518.

Posada, D., Crandall, K.A., 1998. MODELTEST: testing the model of DNA substitution. Bioinformatics 14, 817–818.

Rodriguez, F., Oliver, J.L., Marin, A., Medina, J.R., 1990. The general stochastic model of nucleotide substitution. J. Theor. Biol. 142, 485–501.

Shields, G.F., Adams, D., Garner, G., Labelle, M., Pietsch, J., Ramsay, M., Schwartz, C., Titus, K., Williamson, S., 2000. Phylogeography of mitochondrial DNA variation in brown bears and polar bears. Mol. Phylogenet. Evol. 15 (2), 319–326.

Snyder, J.O., 1912. Japanese shore fishes collected by the United States Bureau of Fisheries steamer "Albatross" expedition of 1906. Proc. U. S. Natl. Mus. 42 (1909), 399–450 51–61.

Swofford, D.L., 2001. PAUP*: Phylogenetic Analysis Using Parsimony (* and Other Methods, version 4.0b10). Sinauer Assoc., Sunderland, MA.

Takishita, K., Inagaki, Y., Tsuchiya, M., Sakaguchi, M., Maruyama, T., 2005. A close relationship between Cercozoa and Foraminifera supported by phylogenetic analyses based on combined amino acid sequences of three cytoskeletal proteins (actin, alpha-tubulin, and beta-tubulin). Gene 5 (362), 153–160.

Tanaka, S., 1931. On the distribution of fishes in Japanese waters. J. Fac. Sci., Imp. Univ. Tokyo, Sec.4, Zool. 3 (1), 1–90 1–3.

Temminck, C.J., and Schlegel, H., 1845. Pisces. Ph. Fr. von Siebold, Fauna Japonica. Part VIII, 133–152, pl. 74.

Yang, Z., 1996. Among-site rate variation and its impact on phylogenetic analyses. TREE 11, 367–372.

Yang, Z., 1997. PAML: a program package for phylogenetic analysis by maximum likelihood. CABIOS 13, 555–556.

Yang, Z., Nielsen, R., Hasegawa, M., 1998. Models of amino acid substitution and applications to mitochondrial protein evolution. Mol. Biol. Evol. 15, 1600–1611.